Ab initio dynamics study of poly-*para*-phenylene vinylene

Guang Zheng,[a] S. J. Clark, P. R. Tulip, S. Brand, and R. A. Abram
Department of Physics, University of Durham, DH1 3LE, United Kingdom

We present an *ab initio* dynamics investigation within a density-functional perturbation theory framework of the properties of the conjugated polymer poly-*para*-phenylene vinylene (PPV) in both the isolated chain and crystalline states. The calculated results show that for an isolated chain, most of the vibrational modes correspond to experimentally observed modes in crystalline PPV. However, additional hitherto unidentified modes have been observed in experiment and our calculations on crystalline material have allowed us to assign these. We also present the results of calculations of the polarizability and permittivity tensors of the material, which are in reasonable agreement with the typical values for conjugated polymers. Dynamical Born effective charges [S. Baroni, S. de Gironcoli, A. Dal Corso, and P. Giannozzi, Rev. Mod. Phys. **73**, 515 (2001)] are calculated and compared with atomic charges obtained from Mulliken population analysis [M. D. Segall, C. J. Pickard, R. Shah, and M. C. Payne, Mol. Phys. **89**, 571 (1996)] and we conclude that effective charges are more appropriate for use in the study of the dynamics of the system. Notable differences are found in the infrared-absorption spectra obtained for the isolated chain and crystalline states, which can be attributed to the differences in the crystalline packing effects, which clearly play a key role in influencing the lattice dynamics of PPV. © *2005 American Institute of Physics*. [DOI: 10.1063/1.1955516]

I. INTRODUCTION

A great deal of interest has been stimulated in conjugated polymers in the last two decades due to their conductive behavior after doping with electron donors or acceptors.[1,2] Considerable attention has also been paid to their undoped state in which the materials demonstrate fascinating semiconducting properties with electronic band gaps ranging from approximately 1 to several eV. As an example, poly-*para*-phenylene vinylene (PPV, Fig. 1) is considered as a typical material since it has a nondegenerate ground state which exhibits good stability and high conductivity after doping. Moreover, it takes the form of quasi-one-dimensional molecules arranged in a three-dimensional crystal structure (Fig. 2) and this arrangement is ideal for studying the properties in different aggregate states. Furthermore, the material is easy to process and there are quite a large number of possible substitutions which give the opportunity to tune the optoelectronic properties. Especially since the discovery of electroluminescence,[3] considerable progress has been made in using the material in displays, light-emitting diodes (LEDs), and field-effect transistors (FETs),[4–6] but there is still more to do to optimize the lifetime of devices.

It is well known that investigation of the dynamical properties (such as vibrational spectra, polarizability, and Born effective charges) of conjugated polymers is one of the most important tools for probing the structural and microscopic optoelectronic properties of the materials in various phases, and in both the pristine and doped states.[7,8] The understanding of the relevant properties requires a detailed knowledge of the dynamical properties. However, it is often

the case that information on the anisotropy of the dynamical properties obtained by different methods has been quite inconsistent.[9] Further, for a large system, the experimental determination of anisotropy is either extremely difficult or only describes the conformational averages. This seriously limits the understanding of the relationship between electronic structure and material properties. Due to the fact that a realistic theoretical description involves heavy computational cost, many calculations of the dynamical properties of polymers have been based either on simple models, such as an isolated, perfectly straight chain where the solid-state effects are not included, or only average axial static properties, while ignoring the anisotropy information. Nevertheless, some recent progress has been made in understanding the dynamical properties for molecules or molecular crystals[10–13] and for conjugated polymers.[14,15] However, uncertainties remain concerning the microscopic basis of chain-chain interactions in the crystalline state. For example, a recent study[16] of the vibrational properties of PPV shows that the calculated phonon modes of an isolated chain are in quite good agreement with the experimental results for a polymer crystal, indicating that the isolated chain model in some circumstances can be a good approximation. However, there are still some experimental vibrational modes which have not been identified in the one chain model, indicating as one would expect that crystalline packing effects are also significant in some cases. Very recently,[17] a theoretical study of dielectric and vibrational properties was carried out, but only for some of the simpler amino acid molecules.

In this work we present an *ab initio* investigation of the dynamical properties of the conjugated polymer PPV. We first focus on the vibrational properties of an isolated PPV

[a] Electronic mail: guang.zheng@durham.ac.uk and gzheng25@yahoo.com
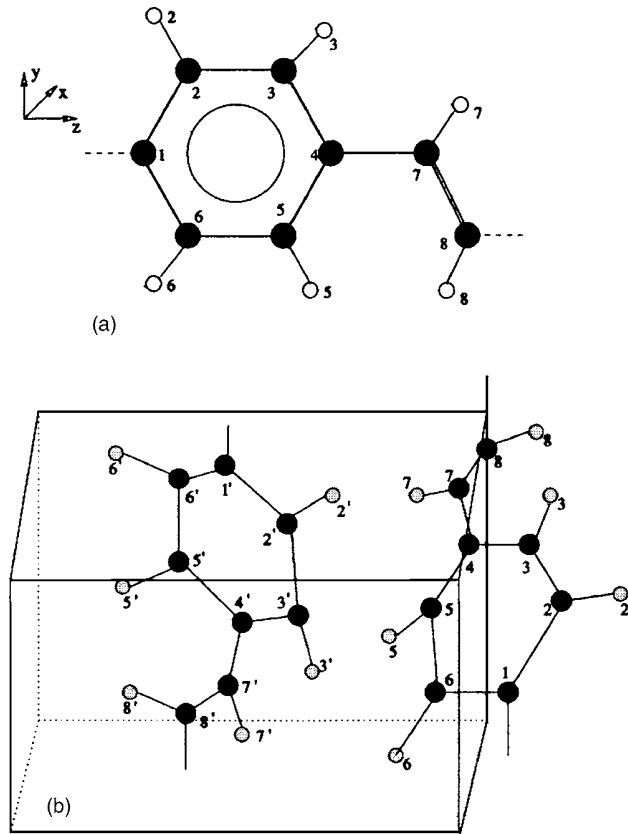
    123, 024904-1

(a)

(b)

FIG. 1. (a) The repeat unit (monomer) of an isolated PPV chain. The black and white circles denote carbon and hydrogen atoms, respectively. The orientation of the PPV with respect to the chosen frame of reference is shown. (b) The numbering scheme for a unit cell of the PPV crystal. The filled and unfilled circles denote carbon and hydrogen atoms, respectively.
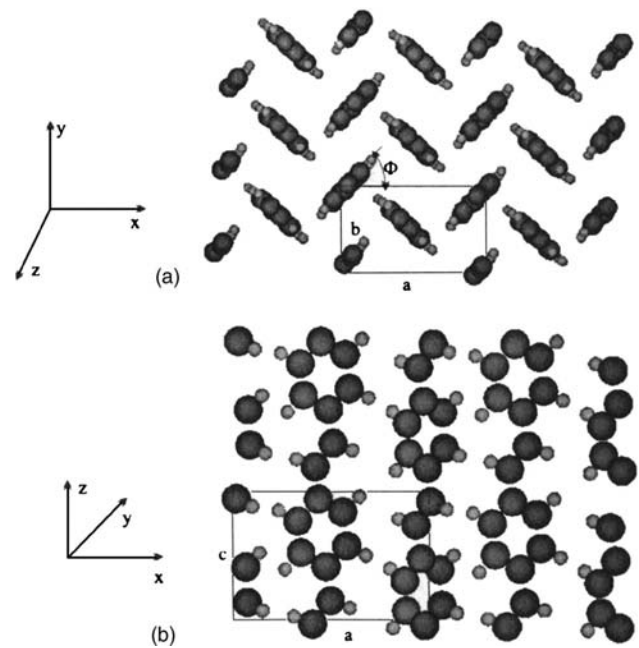

(a)

(b)

FIG. 2. Herringbone crystal structure of PPV (Ref. 26). Polarizabilities quoted are relative to the coordinate system shown in this figure. The monoclinic unit cell has $a=8.07$ Å, $b=6.05$ Å, $c=6.54$ Å, and the angle $\Phi=52°$. (a) Top view of the polymer; (b) side view of PPV.

chain. Then a crystalline state calculation is performed to investigate the unidentified phonon modes seen in experiments on PPV samples. The paper is organized as follows: Sec. II presents the theory and computational details, and then in Sec. III we present the results and their discussion. A short summary concludes the paper in Sec. IV.

II. THEORY AND COMPUTATIONAL DETAILS

According to perturbation theory, when an electric field ϵ is applied, the change of the dipole moment **d** can be written as a power series,

$$d_i - d_{0i} = \alpha_{ij}\epsilon_j + \gamma_{ijk}\epsilon_j\epsilon_k + \cdots, \tag{1}$$

where i, j, and k run over the x, y, and z axes of the system, $\mathbf{d}_0$ is the dipole moment at zero field, α_{ij} is the polarizability tensor, and γ_{ijk} is the first-order hyperpolarizability.

The polarizability tensor α_{ij} may be defined as

$$\alpha_{ij} = \frac{\partial^2 E}{\partial \epsilon_i \, \partial \epsilon_j}, \tag{2}$$

where E is the total energy of the system. Thus the polarizability tensor can be directly evaluated by finding the second-order derivatives of the total energy, which we obtain in this work by the use of linear response, or density-functional perturbation theory (DFPT).[18,19] In practice, we

are only required to know the first-order changes in the charge density and potential in order to evaluate the change in energy to the second order.

We also calculate the components of the polarizability tensor using the finite difference (FD) method, where appropriate. In this method, the change of dipole moment as a function of electric field is obtained and then the coefficients α_{ij} are derived from Eq. (1). However, since the computational cost of the FD method is very considerable and it is not possible to use the method for mixed perturbations, or the response to electric field in crystalline systems, we employ only DFPT for the study of the vibrational properties and effective charges.

DFPT is one of the most robust methods for the calculation of lattice dynamics. It is possible to calculate a number of properties by considering different perturbations. For example, a perturbation of the ionic positions can be used to obtain the dynamical matrix and information on the phonon modes. The squares of the angular frequencies of the phonon modes are the eigenvalues of the dynamical matrix which can be obtained by using a linear-response determination of the second-order change in the total energy induced by atomic displacements,

$$F_{R_iR_j} = \frac{\partial^2 E}{\partial R_i \, \partial R_j}, \tag{3}$$

where E is the vibrational potential energy, and R_i and R_j are the ion coordinates.

The perturbation resulting from an applied electric field allows us to evaluate the dielectric response. The electronic dielectric permittivity tensor β_{ij} is the coefficient of proportionality between the macroscopic displacement field and the macroscopic electric field, in the linear response regime,[18]

TABLE I. The calculated frequencies of the phonon modes (in cm^{-1}) of an isolated PPV chain (1D PPV) at the Γ point obtained in this work. For comparison, other theoretical and experimental results are also listed in the table. "ip" stands for in-plane vibrational modes and "op" indicates out of plane phonon modes. The four unidentified vibrational modes appear as ν_1, ν_2, ν_3, and ν_4 under the description heading.

Symmetry	Description	This work	Calc.[a]	Calc.[b]	Calc.[c]	Expt.[c]	Expt.[b]	Expt.[d]
B_g	op	121.7	147					
A_u	ip	220.9	220	328.1	311	327		
A_g	op	323.9	310					
B_g	op	324.6	327					
A_u	ip	406.2	390	431.2	425	428	429	430
B_u	ip	432.6	430					
A_u	op	553.3	532					556
A_g	ip	639.7	622	619.9	603	634		
A_g	ip	672.6	659	692.3	660	662		
B_g	op	720.9	696					
B_g	op	794.9	785					
B_u	ip	810.6	799	771.5	787	784	785	784
A_u	op	841.2	818					838
B_g	op	882.4	853					
A_g	ip	893.7	899	968.2	896	887	966	963
A_u	op	957.2	911					
B_g	op	963.0	926					
A_u	op	968.2	930					
B_u	ip	1011.2	978	1012.6	1026	1013	1013	1014
B_u	ip	1113.4	1076		1117	1107		1107
	ν_1				1169.9		1178	1180
A_g	ip	1151.3	1111	1174.3	1163	1170	1174	1172
A_g	ip	1208.4	1185		1192	1197		
B_u	ip	1224.7	1187		1181	1179		1194
	ν_2			1205		1210	1211	1211
A_g	ip	1294.3	1262	1303.5	1295	1301	1304	1301
B_u	ip	1296.9	1268	1269.3	1269	1271	1271	1271
A_g	ip	1314.1	1274	1330.1	1330	1329	1327	1329
	ν_3					1302	1302	
B_u	ip	1376.0	1367	1341.1	1333	1340	1339	1340
B_u	ip	1442.2	1458	1416.7	1436	1424	1424	1424
B_u	ip	1505.7	1485	1528.4	1516	1518	1518	1519
	ν_4							1415
A_g	ip	1523.7	1493	1549.6	1538	1546	1550	1547
A_g	ip	1553.1	1546	1586.5	1587	1582	1586	1582
A_g	ip	1637.4	1635	1629.2	1636	1625	1628	1626
A_g	ip	3038.9	2951					
B_u	ip	3051.3	2975	3027.9				
A_g	ip	3074.1	3058					
B_u	ip	3078.3	3064	3065.9				
A_g	ip	3101.2	3116					
B_u	ip	3102.9	3125	3125.1				

[a]Reference 16.
[b]Reference 28.
[c]Reference 27.
[d]Reference 29.

$$\beta_{ij} = \frac{\delta \mathcal{D}_{\text{mac},i}}{\delta \varepsilon_{\text{mac},j}} = \delta_{ij} + 4\pi \frac{\delta \mathcal{P}_{\text{mac},i}}{\delta \varepsilon_{\text{mac},j}}, \qquad (4)$$

$$\beta_{ij}^{\infty} = \delta_{ij} + \frac{4\pi}{\Omega_0} \alpha_{ij}, \qquad (5)$$

where $\mathcal{D}_{\text{mac}}$ is the displacement and $\mathcal{P}_{\text{mac}}$ the polarization. In the limit of low frequencies of the applied field, the electronic contribution to the dielectric permittivity tensor can be written as

where Ω_0 is the volume of the supercell and α_{ij} is the polarizability tensor defined as in Eq. (2). The Born effective charge tensor of the ith ion $Z_{i,jk}^{*}$ is the partial derivative of the macroscopic polarization with respect to a periodic displace-

TABLE II. The calculated and experimental wavelengths (in cm^{-1}) of the four unidentified PPV phonon modes at the Γ point.

Modes	Expt.	Expt.	Theory	This work[a]
ν_1	1178[b]	1176[c]	1169.9[d]	1170.6
ν_2	1211[b]	1210[e,d]	1205[d]	1207.9
ν_3	1302[e]	1302[f]		1297.3
ν_4	1415[f]			1408.9

[a]*Ab initio* calculation for crystalline PPV in this work.
[b]Experimental value from Ref. 28.
[c]Experimental value from Ref. 31.
[d]Theoretical data from effective conjugation coordinate (ECC) in Ref. 28.
[e]Experimental value from Ref. 27.
[f]Experimental value from Ref. 29.

ment of that ion at the limit of zero applied electric field, and in DFPT the tensor is equivalent to the linear relation between the force upon an atom and the applied electric field,[18]

$$Z^*_{i,jk} = \Omega_0 \frac{\delta \mathcal{P}_{\mathrm{mac},j}}{\delta \tau_{ik}} = \frac{\delta F_{ik}}{\delta \varepsilon_j}, \qquad (6)$$

where Ω_0 is the volume of the supercell and τ_{ik} is the displacement of the atom ion i in the direction k.

The Born effective charge is a very important quantity in polar semiconductors and insulators. The long-range behavior of the Coulomb forces gives rise to macroscopic electric fields for longitudinal-optic (LO) phonons at the Γ point and the coupling between longitudinal phonons and the electric field give rise to LO-TO splitting at the Γ point. This splitting is determined by the Born effective charge and by the static dielectric constant of the crystal.[19]

All calculations were performed with the plane-wave pseudopotential implementation of density-functional theory (DFT) using the CASTEP code.[20,21] Plane-wave basis sets have many benefits compared to conventionally used quantum chemistry basis sets; in particular, there exists a simple parameter, the cutoff energy, to determine the completeness of the basis. This gives us confidence that the wave function can describe any properties without bias towards any other particular result.[13] In our calculations, the many-body exchange and correlation interactions are described using the local-density approximation (LDA). Such calculations are capable of giving accurate and reliable structural and electronic information. Norm conserving Kleinman-Bylander[22] pseudopotentials are used to describe the electron-ion interactions. A cutoff energy of 1000 eV is used which converged the total energy of the system to 1.0 meV/cell. The Monkhorst-Pack **k**-point sampling scheme[23] was employed to perform the integrations in **k** space over the first Brillouin zone with the grids for each cell chosen to be dense enough to also converge the total energy to 1.0 meV/cell. In this work, a $1 \times 1 \times 8$ mesh was used for an isolated PPV chain, and 30 **k** points are used for the crystalline state. The threshold value of the ionic forces is 0.05 eV/Å^3. The Kerker density-mixing scheme[24] was used to achieve self-consistency.

The use of a plane-wave basis set requires periodic boundary conditions in all three dimensions. To achieve this the PPV chain was artificially repeated in the two dimensions
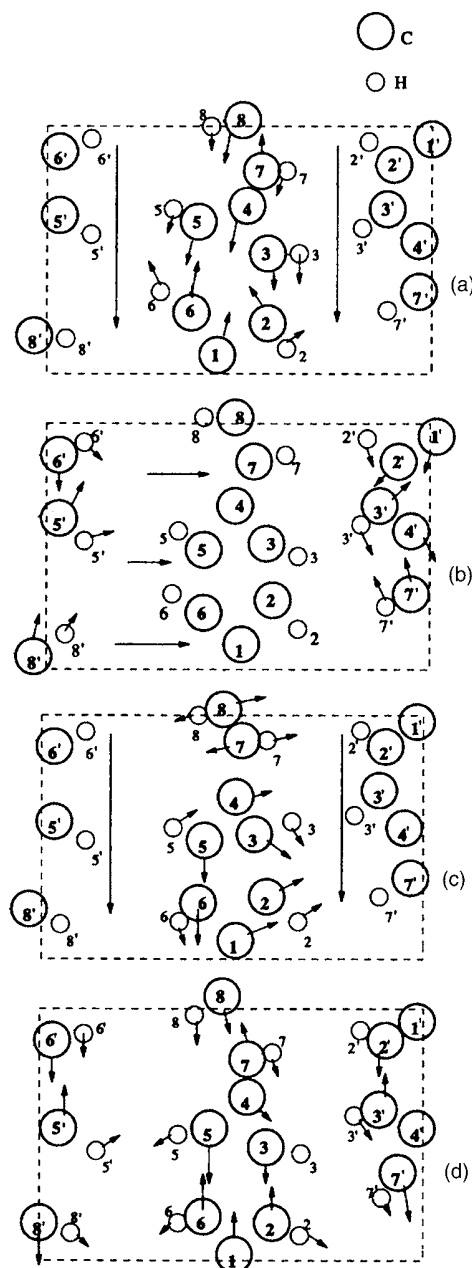

FIG. 3. Representation of the atomic displacements of PPV in a unit cell in the crystalline state. At a particular time t, the vibration direction is shown by the arrows. Shown are the calculated phonon modes at (a) 1170.6 cm^{-1}, (b) 1207.9 cm^{-1}, (c) 1297.3 cm^{-1}, and (d) 1408.9 cm^{-1}.

normal to the polymer axis with a sufficiently large unit cell to make neighboring interactions negligible. For an isolated PPV chain, the unit cell dimension is $15 \times 15 \times d$ Å^3, where d is the repeat distance along the polymer chain. In our calculations, the ground-state lattice constant d is found to be 6.65 Å, and the torsion configuration of the polymer is planar.[25] For a detailed study of the geometrical properties, the readers are referred to Ref. 25. In the solid state of PPV, we calculate a herringbone crystal structure,[26] with $a = 8.07$ Å, $b = 6.05$ Å, and $c = 6.54$ Å, the monoclinic angle between b and c is 123°, the setting angle Φ is 52° (Fig. 2), and the unit cell has $P2_1/a$ symmetry.

TABLE III. The calculated polarizabilities α^{DFPT} and α^{FD} (in Å^3) and permittivity (β) tensor components for a PPV isolated chain (1D PPV) and the crystalline state. β is calculated using Eq. (5). $\alpha_{\mathrm{av}}^{\mathrm{FD}}$ is calculated using the FD method for a styrene molecule, which is formed by saturating the two dangling bonds with hydrogen atoms in the PPV monomer shown in Fig. 1. α_{av} and β_{av} are Tr(α)/3 and Tr(β)/3, respectively.

	α^{DFPT}			$\alpha_{\mathrm{av}}^{\mathrm{DFPT}}$		α^{FD}			$\alpha_{\mathrm{av}}^{\mathrm{FD}}$
1D PPV	7.54	−0.05	0.09		Styrene	18.9	−1.72	0.02	
	−0.05	14.49	−1.64			−1.72	34.1	−0.09	
	0.09	−1.64	160.56	60.8		0.02	−0.09	45.3	32.8
Crystal	37.65	−0.06	−3.39						
	−0.06	31.94	0.005						
	−3.39	0.005	110.81	60.1					
	β			β_{av}	Polythiophene[a]	β			β_{av}
1D PPV	1.14	−0.009	0.002						
	−0.009	1.27	−0.031						
	0.002	−0.031	4.03	2.15					
Crystal	2.76	−0.003	−0.159		PT crystal[a]	2.6			
	−0.003	2.49	0.00				3.3		
	−0.159	0.00	6.19	3.8				10.8	5.6

[a]*Ab initio* calculation for crystalline polythiophene (PT) (Ref. 33).

III. RESULTS AND DISCUSSION

A. Vibrational properties

The vibrational properties of PPV have been previously studied, both theoretically and experimentally, by a number of groups.[16,27–29] In the present work we calculate vibrational normal-mode frequencies and displacements by directly evaluating the matrix of force constants using DFPT. Table I shows our calculated vibrational frequencies at the Γ point for a PPV chain, along with previously published results. We adopt the symmetry labeling of Refs. 16 and 28 based on the C_{2h} point group. Table I shows that the frequencies of the ring C–C stretch modes are in the range of 1314.1–1553.1 cm^{-1}, while the vinylene stretch frequency is at 1637.4 cm^{-1}, close to the experimental value.[30] These results are in good agreement with other theoretical and experimental data.[16,28,29] The higher-frequency phonon modes (from 3038.9 to 3102.9 cm^{-1}) are due to C–H stretch vibrations. It is found that most of the out-of-plane modes are softer than the in-plane ones, since the former mainly involve bond-length and bond-angle alternations.

The results of the isolated chain calculations are in very good agreement with recent publications, and it is possible to assign most of the experimental vibrational frequencies. However, there are still four experimental modes denoted as ν_1, ν_2, ν_3, and ν_4 in Table I which are not assigned by the isolated chain model calculation.[16] To see whether those modes derive from the crystalline nature of the measured samples, we have performed calculations for crystalline PPV and have found that the four experimental frequencies are successfully reproduced in our calculation, as shown in Table II. The atomic displacements of PPV in a crystalline unit cell are illustrated in Fig. 3. The main feature of the vibrations is that all of them involve neighboring chain-chain interactions. Especially for some hydrogen atoms, direct hydrogen-hydrogen interactions seem to exist. A feature of the 1170.6-cm^{-1} mode [in Fig. 3(a)] is that all the atoms in the two neighboring chains vibrate in the same direction, and in the central chain, all the atoms vibrate in the central plane. At

a particular time, the vibration direction of each individual atom is shown in the corresponding figure. In the case of the 1207.9-cm^{-1} mode [Fig. 3(b)], the atoms in the central chain vibrate out of the central plane. The properties of the 1297.3-cm^{-1} vibration are similar to that of the 1170.6-cm^{-1} mode; the atoms in the two neighboring chains move in the same direction. In the central chain, there exist stretch vibrations with a larger amplitude between both phenyl and vinyl atoms. For the 1408.9-cm^{-1} mode, the stretching vibrations exist in the two chains in the unit cell. The correlated motion of the modes seen only in crystalline material suggests that interchain interactions play a key role in determining their frequencies.

B. Polarizability and permittivity

We have also carried out calculations of the polarizability α and permittivity β tensors of PPV. Figure 1 shows the coordinate system used to define the tensors relative to an isolated polymer chain. The z direction is shown in Fig. 1, and the x and y directions are, respectively, perpendicular and parallel to the plane of the phenyl ring. For the crystalline state, the orientations of the polymer chains are shown in Fig. 2. Two distinct methods have been employed for the calculation of the polarizability of PPV: one is linear-response DFPT and the other is the FD-DFT approach, which has been shown[13] to be capable of yielding values in good agreement with experiment for molecules. The polarizability and the permittivity tensor components calculated using DFPT are given in Table III. For comparison, we have also calculated the FD-DFT polarizability for a styrene molecule, which is realized by saturating the two dangling bonds with hydrogen atoms in the PPV repeat unit shown in Fig. 1. The calculated dipole moment as a function of applied field is shown in Fig. 4. An analysis of the individual components of the induced dipole moment as a function of electric field gives the relevant polarizability tensor components listed in Table III.

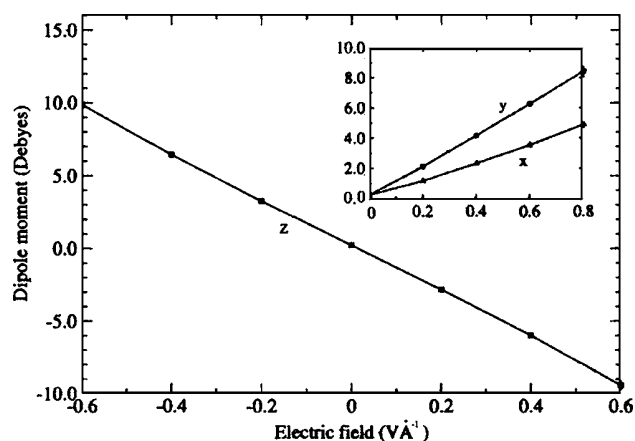As the experimental determination of the full polariz-

FIG. 4. The magnitude of the induced molecular dipole moment for styrene as a function of an external electronic field applied in the z direction. In the inset are the responses to the x and y components of dipole with respect to x and y fields, respectively. The individual components of the dipole moment are used to determine elements of the polarizability tensor.
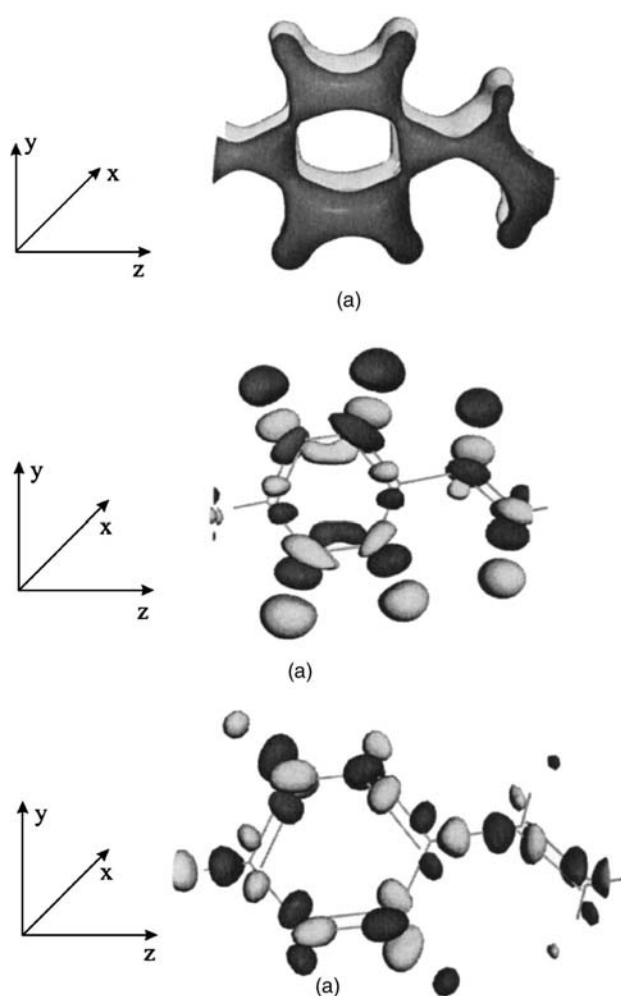

FIG. 5. The first-order electronic charge densities (i.e., the first-order variation in the charge densities resulting from the perturbing potential) for an isolated PPV chain. (a), (b), and (c) correspond to perturbations in the x, y, and z directions, respectively. The dark represents positive charge displacement, and light negative.

ability tensor information is rather difficult, it is instructive to compare the DFPT results with the corresponding finite difference results of styrene. It is found that α^{DFPT} for the polymer is much more anisotropic than for styrene. The results show that there is a major difference between relevant values in the polymer and styrene. For the molecular case, the diagonal components of α are much less anisotropic than for one-dimensional (1D) PPV. For an isolated PPV chain, as can be seen in Table III, the major contribution to the average of polarizability $\alpha_{\text{av}}^{\text{DFPT}} = \text{Tr}(\alpha^{\text{DFPT}})/3$ is the component α_{zz} in the z direction. Our value of $\alpha_{\text{av}}^{\text{DFPT}}$ is reasonable when compared with typical data for the axial polarizability for conjugated polymers.[14,15] However, there is currently no other similar work on the anisotropy of polarizability which we can use for comparison. It is apparent that $\alpha_{zz} \gg \alpha_{yy}$ and $\alpha_{yy} \sim \alpha_{xx}$ for both the isolated chain and crystalline states. Although the three principal components differ from those of an isolated chain, $\alpha_{\text{av}}^{\text{DFPT}}$ is very similar for the crystalline state.

The diagonal elements of the electronic permittivity of PPV also show quite strong anisotropy with $\beta_{zz} \gg \beta_{yy}$ and $\beta_{xx} \simeq \beta_{yy}$. The predicted value of the average of PPV permittivity β_{av} is in good agreement with the typical permittivity value of approximately 3.[32] A similar permittivity anisotropy can be found for crystalline polythiophene (PT).[33] In both PPV and PT, the permittivity principal component value β_{zz} is much larger than those in the other directions.

The linear response of the electronic charge density to the applied electric field can be visualized by making a plot of the first-order perturbation of the charge density, which is the linear (i.e., first order) variation in the electronic charge density resulting from the perturbing potential. The simple way to regard it for an electric field is to consider how the charge density would vary under application of the field, i.e., where the electrons would flow from and where they would flow to. The first-order density obtained by the DFPT treatment is plotted in Fig. 5 and it is found that the density corresponding to the perturbations in the x axis are highly

polarized. A more quantitative analysis of this response can be gained by examination of the effective charges on the constitute atoms.

C. Born effective charge

In Table IV, the principal components of the Born effective charge tensors for an isolated chain and crystalline states of PPV, together with atomic charges obtained by Mulliken population[34] analyses, are presented. Note that we show the charges for symmetry-related atoms in the table. In the calculations we do not enforce symmetry so as to investigate if any symmetries are broken (we find that none are). The slight differences in charges on symmetry-related atoms indicate the computational accuracy of the data presented (approximately two decimal places). It is found that all the Mulliken population atomic charges, except for certain carbon atoms, possess roughly the same value for each atom type (H or C) in both the isolated chain and the crystal. This suggests that the electronic structure of each atom is similar regardless of the two different packing states. However, discrepancies exist between the Mulliken atomic charges and the average

TABLE IV. The trace of the Born effective charge tensor $Z_{\alpha\beta}^*$ for both an isolated PPV chain (1D PPV) and the crystalline state, together with the Mulliken atomic population charges. Z_{av}^* is the trace/3 of the effective charge principal components. Z_{at} is the atomic charge from Mulliken population analysis. All the values are in units of e.

1D PPV			Crystal					
Atom	Z_{av}^*	Z_{at}	Atom	Z_{av}^*	Z_{at}	Atom	Z_{av}^*	Z_{at}
H_2	0.046	0.30	H_2	0.131	0.28	H_2'	0.134	0.27
H_3	0.038	0.31	H_3	0.100	0.27	H_3'	0.097	0.27
H_5	0.046	0.30	H_5	0.157	0.26	H_5'	0.159	0.26
H_6	0.037	0.31	H_6	0.084	0.26	H_6'	0.082	0.27
H_7	0.062	0.27	H_7	0.084	0.27	H_7'	0.085	0.27
H_8	0.041	0.27	H_8	0.067	0.26	H_8'	0.065	0.25
C_1	0.154	−0.02	C_1	0.201	−0.03	C_1'	0.198	−0.03
C_2	−0.113	−0.29	C_2	−0.155	−0.24	C_2'	−0.158	−0.24
C_3	−0.209	−0.29	C_3	−0.145	−0.28	C_3'	−0.147	−0.28
C_4	0.188	−0.02	C_4	0.173	−0.03	C_4'	0.176	−0.02
C_5	−0.113	−0.29	C_5	−0.120	−0.22	C_5'	−0.122	−0.22
C_6	−0.193	−0.29	C_6	−0.114	−0.27	C_6'	−0.117	−0.27
C_7	0.005	−0.28	C_7	0.095	−0.25	C_7'	0.095	−0.26
C_8	0.043	−0.28	C_8	0.034	−0.28	C_8'	0.033	−0.28

dynamical Born effective charges. For hydrogen atoms in the crystal, there are marked differences between the average Born effective charges and the atomic population charges. For an isolated chain the discrepancies are even more marked, with the effective charges being only about one-tenth of the Mulliken charges. For the carbon atoms, there are clear disagreements; there are different charge signs for atoms C_1, C_4, C_7, and C_8 in the isolated chain and for C_1, C_4, C_7, C_8, C_1', C_4', C_7', and C_8' in the crystalline state. It is noted that the alpha carbons C_1 and C_4 for an isolated PPV chain; C_1, C_4, C_1', and C_4' for PPV crystal) have almost no Z_{at} charge and quite some positive Z_{av}^* charges. The polar distribution of charges for alpha carbons may be responsible for the differences of Z_{av}^* for the equivalent atoms C_7 and C_8 for the 1D PPV. It would be gratifying to confirm this from direct experiments.

The discrepancies between the effective charges and population atomic charges highlight their different origins. The Mulliken population charges are based on the partition of the Kohn-Sham orbitals and provide information on the static electronic structures, whereas the Born effective charges are based upon the dynamics of the system, and provide information concerning dynamical properties. Therefore when a dynamical property is involved, effective charges are normally more appropriate for use in the study of the physics of the system.

The infrared (IR) absorption coefficient can be expressed as[17]

$$I_m \propto \sum_{\alpha} |\sum_{\kappa,\beta} Z_{\kappa,\alpha\beta}^* e_m(\kappa\beta)|^2, \qquad (7)$$

where m is the mode of vibration, $Z_{\kappa,\alpha\beta}^*$ is the effective charge, and e_m is the phonon eigenvector. For complex systems such as conjugated polymers, the IR spectrum can be helpful and very useful in interpreting the vibrational properties. The calculated IR spectrum of an isolated chain is plotted in Fig. 6, and for a crystal in Fig. 7. Due to there

being two chains per unit cell there are more peaks in Fig. 7. The peaks in the IR spectrum for crystalline state are shifted and broadened when compared with that of Fig. 6, especially in the region in which the four unidentified modes lie (that is from 1170.6 to 1408.9 cm^{-1}); there is a big relative increase for the IR absorption in that region. These differences can be attributed to interchain interactions in the crystalline state. In addition, in the crystalline calculation there is an absorption peak at 2078.3 cm^{-1} which originated from asymmetric vibrations among the atoms shown in the inset of Fig. 7, which has not been reported in experiments.

IV. CONCLUSION

We have presented an *ab initio* dynamics investigation of the properties of the conjugated polymer poly-*para*-phenylene vinylene in both the isolated chain and crystalline states. We have calculated the vibrational properties of PPV by directly evaluating the dynamical matrix of force constants using a DFPT determination of the second-order
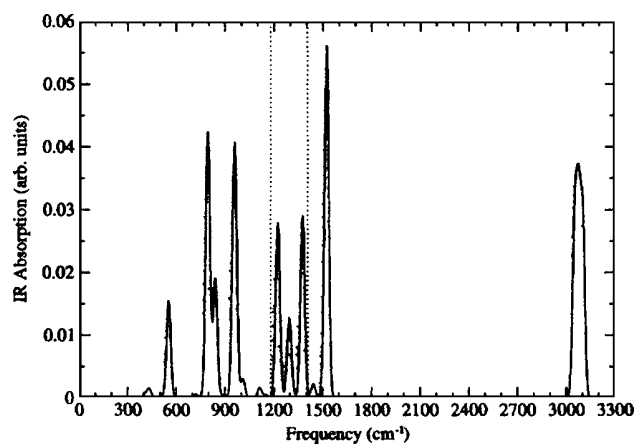

FIG. 6. IR absorption spectrum for an isolated PPV polymer chain. The absorption spectrum has been Gaussian broadened at $T = 300$ K.
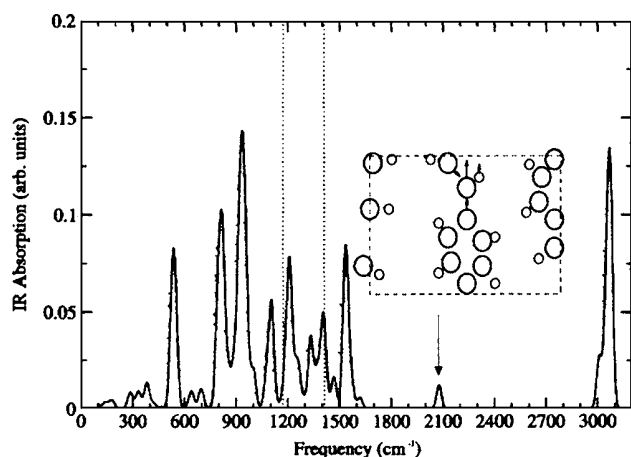
FIG. 7. IR spectrum for crystalline PPV state. Gaussian broadening at $T = 300$ K has been used on the absorption spectrum. The inset is a snapshot of the calculated 2078.3-cm^{-1} frequency mode which is due to asymmetric vibrations of the atoms shown.

change in the total energy induced by atomic displacements. We found that most of the vibrational frequencies in an isolated PPV chain can be associated with specific modes seen in experimental studies of crystalline PPV. The higher-frequency phonon modes are due to the C–H stretch, while the vinyl C–C stretch mode has a higher frequency than the phenyl ring C–C stretch modes. Calculations for the crystalline state allow us to assign several previously unidentified experimentally observed modes which are not seen in the isolated chain calculation. Information has also been obtained on the polarizability and permittivity tensors of the PPV. The results are in reasonable agreement with typical values of the axial polarizability and permittivity of conjugated polymers. Analyses of the first-order electronic charge densities give insight into the behavior of the electronic polarizability. Dynamical Born effective charges have been calculated and compared with the Mulliken population atomic charges. Although there are differences, it is argued that effective charges are more appropriate for use in the study of the dynamics of the system. Notable differences are found in the predicted IR absorption spectra obtained for an isolated chain and PPV in the crystalline state. The results demonstrate that the chain-chain interactions in the crystal play a key role in determining the dynamical properties.

ACKNOWLEDGMENTS

[1] C. K. Chiang, M. A. Druy, S. C. Gau, A. J. Heeger, E. J. Louis, A. G. MacDiarmid, Y. W. Park, and H. Shirakawa, J. Am. Chem. Soc. **100**, 1013 (1978).

[2] C. K. Chiang, C. R. Fincher, Y. W. Park, A. J. Heeger, H. Shirakawa, E. J. Louis, S. C. Gau, and A. G. MacDiarmid, Phys. Rev. Lett. **39**, 1098 (1977).

[3] J. H. Burroughes, D. D. C. Bradley, A. R. Brown, R. N. Marks, K. Mackay, R. H. Friend, P. L. Burns, and A. B. Holmes, Nature (London) **347**, 539 (1990).

[4] G. H. Gelinck, T. C. T. Geuns, and D. M. de Leeuw, Appl. Phys. Lett. **77**, 1487 (2000).

[5] C. J. Drury, C. M. J. Mutsaers, C. M. Hart, M. Matters, and D. M. de Leeuw, Appl. Phys. Lett. **73**, 108 (1998).

[6] F. Hide, M. A. Diaz-Garcia, B. J. Schwartz, M. R. Andersson, Q. Pei, and A. J. Heeger, Science **273**, 1833 (1996).

[7] S. Califano, *Vibrational States* (Wiley, New York, 1976).

[8] G. Zerbi, in *Advances in Infrared and Raman Spectroscopy*, edited by R. J. H. Clark and R. E. Hester (Wiley-Heyden, New York, 1984).

[9] *The Optics of Thermotropic Liquid Crystals*, edited by S. Elston and R. Sambles (Taylor & Francis, London, 1998).

[10] C. J. Adam, S. J. Clark, G. J. Ackland, and J. Crain, Phys. Rev. E **55**, 5641 (1997).

[11] S. J. Clark, C. J. Adam, G. J. Ackland, J. White, and J. Crain, Liq. Cryst. **22**, 469 (1997).

[12] S. J. Clark, C. J. Adam, D. J. Cleaver, G. J. Ackland, and J. Crain, Liq. Cryst. **22**, 477 (1997).

[13] S. J. Clark, G. J. Ackland, and J. Grain, Europhys. Lett. **44**, 578 (1998).

[14] M. van Faassen, P. L. de Boeij, R. van Leeuwen, J. A. Berger, and J. G. Snijders, Phys. Rev. Lett. **88**, 186401 (2002).

[15] P. Mori-Sánchez, Q. Wu, and W. Yang, J. Chem. Phys. **119**, 11001 (2003).

[16] R. B. Capaz and M. J. Caldas, Phys. Rev. B **67**, 205205 (2003).

[17] P. R. Tulip and S. J. Clark, J. Chem. Phys. **121**, 5201 (2004).

[18] X. Gonze, Phys. Rev. B **55**, 10337 (1996); X. Gonze and C. Lee, Phys. Rev. B **55**, 10355 (1996).

[19] S. Baroni, S. de Gironcoli, A. Dal Corso, and P. Giannozzi, Rev. Mod. Phys. **73**, 515 (2001).

[20] M. C. Payne, M. P. Teter, D. C. Allan, T. A. Arias, and J. D. Joannopoulos, Rev. Mod. Phys. **64**, 1045 (1992).

[21] M. D. Segall, P. J. D. Lindan, M. J. Probert, C. J. Pickard, P. J. Hasnip, S. J. Clark, and M. C. Payne, J. Phys.: Condens. Matter **14**, 2717 (2002).

[22] L. Kleinman and D. M. Bylander, Phys. Rev. Lett. **48**, 1425 (1982).

[23] H. J. Monkhorst and J. D. Pack, Phys. Rev. B **13**, 5188 (1976).

[24] Kerker mixing recognizes the fact that small-*G* components of the charge density should be mixed with smaller weighting in order to prevent charge "sloshing" during SCF optimization.

[25] G. Zheng, S. J. Clark, S. Brand, and R. A. Abram, J. Phys.: Condens. Matter **16**, 8609 (2004).

[26] D. Chen, M. J. Winokur, M. A. Masse, and F. E. Karasz, Phys. Rev. B **41**, 6759 (1990).

[27] J. Orion, J. P. Buisson, and S. Lefrant, Phys. Rev. B **57**, 7050 (1998).

[28] B. Tian, G. Zerbi, and K. Müllen, J. Chem. Phys. **95**, 3198 (1991).

[29] A. Sakamoto, Y. Furukawa, and M. Tatsumi, J. Phys. Chem. **96**, 1490 (1992).

[30] S. J. Martin, D. D. C. Bradley, P. A. Lane, H. Mellor, and P. L. Burn, Phys. Rev. B **59**, 15133 (1999).

[31] D. D. C. Bradley, J. Phys. D **20**, 1389 (1987).

[32] J. W. van der Horst, P. A. Robert, M. A. J. Michaels, and H. Bässler, J. Chem. Phys. **114**, 6950 (2001).

[33] J. W. van der Horst, P. A. Robert, P. H. L. de Jong, M. A. J. Michaels, G. Brocks, and P. J. Kelly, Phys. Rev. B **61**, 15817 (2000).

[34] M. D. Segall, C. J. Pickard, R. Shah, and M. C. Payne, Mol. Phys. **89**, 571 (1996); M. D. Segall, R. Shah, C. J. Pickard, and M. C. Payne, Phys. Rev. B **54**, 16317 (1996).